Raman scattering by the coupled plasmon–LO-phonon modes near the $E_0+\Delta_0$ gap of n-type GaAs: Resonance and interference effects

V. Vorlíček and I. Gregora
Institute of Physics, Czechoslak Academy of Sciences, Cukrovarnická 10, CS-162 00 Praha 6, Czechoslovakia

W. Kauschke
Department Grundlagenentwicklung Halbleitertechnik, Drägerwerk A.G., Moislinger Allee 53-55, D-2400 Lübeck, Federal Republic of Germany

J. Menéndez
Department of Physics, Arizona State University, Tempe, Arizona 85287-1504

M. Cardona
Max-Planck-Institut für Festkörperforschung, Heisenbergstrasse 1, Postfach 80 06 65, D-7000 Stuttgart 80, Federal Republic of Germany
(Received 14 May 1990)

The semiclassical model of Klein, extended to the case of an absorbing medium, is used to discuss Raman scattering by coupled plasmon–LO-phonon modes in n-type GaAs near the $E_0+\Delta_0$ gap. A reasonably quantitative agreement between the calculated and measured squared Raman polarizabilities is found below resonance, whereas additional assumptions are necessary to achieve comparable results above it. Exactly at resonance, the model predicts a behavior somewhat different from the observed one.

I. INTRODUCTION

The investigation of interference effects in resonance Raman scattering (RRS) by longitudinal excitations in zinc-blende-type semiconductors has helped considerably in understanding the role of the particular mechanisms in the scattering process.[1,2] Dipole-forbidden (symmetry Γ_1) as well as dipole-allowed (symmetry Γ_{15}) mechanisms contribute to scattering near reosnance. Only the intrinsic forbidden mechanism, however, is related to the same final states in $\mathbf{q}$ space as the dipole-allowed one and may therefore interfere with it. Thus, a separation between extrinsic and intrinsic scattering becomes, in principle, possible. These effects have been observed near the $E_0+\Delta_0$, E_1, and $E_1+\Delta_1$ gaps in many III-V compound semiconductors. The well-established theory of RRS by LO phonons which assumes the free-electron-hole pairs as intermediate states in the scattering process has been used for the interpretation of experimental results near the $E_0+\Delta_0$ gap (see Ref. 3 for a recent review). For the E_1 and $E_1+\Delta_1$ gap regions, the current theories have been reformulated and generalized to cover the scattering by both LO phonons and plasmons.[2] Recently, a theory of one-phonon Raman scattering which takes into account the correlated electron-hole pairs as intermediate states (excitonic effects) has been developed and applied successfully to the experimental spectra reported for the E_0 and $E_0+\Delta_0$ gaps of GaAs, GaP, and InP.[4]

The deformation potential (DP), together with the interband Fröhlich or electro-optic (EO) interaction, provide the dipole-allowed mechanism for the scattering by LO phonons which interferes with the intraband Fröhlich (F) process. Similarly, the EO and F mechanisms interfere in the scattering process by plasmons near the E_1, and $E_1+\Delta_1$ gaps.[2] The most complex case is that of the coupled plasmon–LO-phonon modes near the E_0 and $E_0+\Delta_0$ gaps for semiconductors with carriers at Γ: Here, all the above-mentioned mechanisms are effective, in addition to the charge-density fluctuations (CDF's).[5–7]

Experimentally, the interference is manifested in apparent anomalies of selection rules when measuring in different configurations, e.g., on the (001) face. Throughout this paper we shall deal with the following configurations:

$$\begin{aligned}&\text{(I)}\ \ \bar{z}(x',x')z\ ,\\ &\text{(II)}\ \ \bar{z}(y',y')z\ ,\\ &\text{(III)}\ \ \bar{z}(x,x)z\ ,\\ &\text{(IV)}\ \ \bar{z}(y,x)z\ .\end{aligned}\tag{1}$$

Here, we adopt the notation x, y, z, x', and y' for the [100], [010], [001], [110], and [1$\bar{1}$0] directions, respectively, introduced in Ref. 1. Since the $z,\bar{z}$ directions are common to all configuration symbols in (1), they will be dropped in what follows.

RRS by coupled plasmon–LO-phonon modes near the $E_0+\Delta_0$ gap in n-type GaAs has been reported by Pinczuk *et al.*[8] The resonance curves observed for the configuration (x,x), where the DP and EO mechanisms are not effective, were explained semiquantitatively by the CDF and F mechanisms. Chen[9] showed that the interfer-

ence between the DP, EO, and CDF mechanisms also explains qualitatively the apparent anomaly of the Raman spectra taken in the (x',x') and (y',y') configurations. However, no resonance profiles were given in Ref. 9, as the measurements were carried out with discrete red lines of the Kr-ion laser. Thus, although the interference effects in Raman scattering by coupled plasmon–LO-phonon modes in n-type GaAs have been known for a long time, no detailed study of the interference curves [analogous to that reported for intrinsic GaAs (Refs. 1 and 10)] has been performed so far.

The present paper aims to fill this gap in the literature. The spectral line shapes are successfully modeled using the semiclassical dielectric theory developed by Klein *et al.*,[5] which has been generalized to the case of an absorbing medium. Making use of the well-established expressions for resonant Raman scattering by LO phonons, we also calculate the resonance profiles expected within the framework of this model. Very good agreement with experiment is found below resonance, whereas additional assumptions are necessary to achieve the same above it. At the resonance itself, a remarkable discrepancy is seen. Arguments are given to the effect that both the crudeness of the model and the character of the sample used are responsible for this discrepancy.

III. THEORETICAL BACKGROUND

The differential Raman efficiency per unit length, for light scattered into the solid angle $\partial\Omega$ and frequency interval $\partial\omega_S$, may be written as[5]

$$\frac{\partial^2 S}{\partial\Omega\,\partial\omega_S}=\frac{1}{(4\pi)^2}\frac{\omega_S\omega_L}{c^4}\frac{n_S}{n_L}\frac{1}{Z^2}\frac{\hbar}{\pi}\times[1+n(\Omega)]\sum_{j,k} d_j^* d_k \mathrm{Im}\chi_{jk} \ . \tag{2}$$

$j(k)=1,2$, where ω_L (ω_S) is the frequency of the incident (scattered) light, n_L (n_S) the refractive index at the incident (scattered) frequency, $n(\Omega)$ the occupation number of the longitudinal mode with frequency Ω, and Z the effective charge associated with the displacement belonging to the mode. The generalized susceptibilities χ_{jk} are related to the phonon (χ_1) and plasmon (χ_2) contributions to the total dielectric function ϵ by

$$\chi_{jk}=\chi_j(\delta_{jk}-\chi_k/\epsilon) \ . \tag{3}$$

We shall use the hydrodynamical model[11] for the susceptibility χ_2 and its spatial dispersion. It has been found that this approach gives basically the same results as the more general Lindhard-Mermin theory, provided that Landau damping is negligible.[7,11]

The quantities d_1 and d_2 in (2) are the total Raman tensors for the modes of Γ_{15} (allowed) and Γ_1 (forbidden) symmetry, respectively, contracted between the incident and scattered polarization vectors $\mathbf{e}_L$ and $\mathbf{e}_S$:

$$d_1=\mathbf{e}_S\cdot(\underline{\mathbf{R}}_{\mathrm{DP}}+\underline{\mathbf{R}}_{\mathrm{EO}})\cdot\mathbf{e}_L \ , \tag{4a}$$

$$d_2=\mathbf{e}_S\cdot(\underline{\mathbf{R}}_{F}+\underline{\mathbf{R}}_{\mathrm{CDF}})\cdot\mathbf{e}_L \ . \tag{4b}$$

The tensors in d_2 are diagonal and those in d_1 are off diagonal with respect to the crystallographic axes; for scattering on the (001) face, they have a very simple structure (see, e.g,. Ref. 1). The independent components of the Raman tensors are the Raman polarizabilities a.

The Raman polarizabilities involved in (4a) and (4b) are generally complex in the intrinsic absorption region. Thus, interference between them is possible, as seen from Eq. (2), especially in the vicinity of a resonating electronic gap, where both real and imaginary parts of the individual polarizabilities are of the same order of magnitude.

The expressions for the dispersion of Raman polarizabilities for LO phonons near the $E_0+\Delta_0$ gap are summarized in Ref. 12. To our knowledge, no rigorous derivation of the Raman polarizabilities for the coupled plasmon–LO-phonon modes has been published so far. Making use of the general considerations reported in Ref. 7, we arrive at a generalization of the results of Ref. 5 for the CDF mechanism near the E_0 and $E_0+\Delta_0$ gaps:

$$a_{\mathrm{CDF}}=-i\left\{A+\frac{eZq}{\omega_L\omega_S m}\left[1+\frac{1/m_c-1}{2/\bar{E}_0+1/E_G}\left[\frac{2\bar{E}_0}{(\bar{E}_0-i\eta_0)^2-(\hbar\omega_L)^2}+\frac{E_G}{(E_G-i\eta_G)^2-(\hbar\omega_L)^2}\right]\right]\right\} , \tag{5}$$

where $\bar{E}_0$ and E_G denote the E_0 and the $E_0+\Delta_0$ gap, respectively, corrected for band filling due to the presence of free electrons (Burstein-Moss shift plus renormalization) and q conservation during the process, and m_c denotes the electron effective mass at the Fermi energy. The phenomenological Lorentzian broadening η has been included to represent the finite lifetime of the electronic states and to avoid the undesired singularities at the gaps. The constant term A is a parameter that has to be determined from a fit to the experimental data. Of course, for $\hbar\omega_L$ well below E_0, a_{CDF} is pure imaginary

III. EXPERIMENT

A. Experimental details

The samples of n-type GaAs used for the present study were cut from a (001)-oriented commercial Czochralski-grown wafer (Wacker Chemistronics, Burghausen, FRG). The (001) face was carefully mechanically and chemically polished. Three rectangular slabs with the longer edges parallel to the x, x', and y' directions were prepared. The x' and y' directions were checked by inspection of

TABLE I. Carrier concentration N and plasma-damping constant of the samples used.

Sample	N (10^{18} cm^{-3}) ir	N (10^{18} cm^{-3}) Raman	Γ (meV) Raman
(x',x')	1.5	1.45	6.8
(y',y')	1.3	1.29	7.5
(x,x), (y,x)	1.7	1.55	8.7

the etch pattern.[1] Their nominal free-electron concentration was determined from ir-reflectivity measurements[13] to be $(1.5\pm0.2)\times10^{18}$ cm^{-3} (cf. Table I). The sample-substitution method with high-purity silicon as a reference sample was used to determine the absolute values of the Raman efficiency and of the squared Raman polarizability taking into account the dispersion of the Raman polarizability (and efficiency) of Si.[14] Details of this procedure are described in Refs. 1 and 10.

The measurements were performed at 100 K, in the spectral range 1.8–2.06 eV. The spectra were excited by the red lines of a Kr^+ laser and by cw dye lasers with the dyes DCM [4-(dicyanomethylene)-2-methyl-6-(*p*-dimethyl-amino-styryl)-4*H*-pyrane] and Rhodamine-6G (Lambda Physik, Göttingen) pumped with all lines of an Ar^+ laser. Both Jarrell-Ash 1.85–2.06 eV) and SPEX Industries, Inc. (1.8–1.916 eV) double-grating monochromators equipped with holographic gratings followed by a RCA 31034 photomultiplier operating in a standard photon-counting mode were used to analyze the scattered light.

B. Experimental results

The spectra measured in the four configurations (1) at $\hbar\omega_L = 1.8$ eV (well below the resonance) are shown in Fig. 1(a). Corresponding calculated spectra of the L^- and L^+ modes are shown in Fig. 1(b) (see Sec. IV A). A pronounced difference is seen between the configurations (x',x') and (y',y'), indicating the presence of the interference effect.[9] In addition to the coupled plasmon–LO-phonon modes L^- and L^+, the peaks at the "undoped" TO- and LO-phonon frequencies are also seen; the latter must originate at the surface-depletion layer. The appearance of the TO peak is only partly explained by the deviations from ideal alignment in the real experiment (the scattered light is always collected from a finite solid angle). The breakdown of the q-selection rule caused by the impurities, especially in the depleted layer where they are unscreened, is probably responsible for this effect, in analogy with the case of heavily doped p-type GaAs.[15] The absence of this feature in the configuration (x,x) would imply deformation-potential coupling to phonons which vibrate in the same direction as the allowed LO phonons, but are made transverse through impurity scattering.

With increasing laser frequency ω_L, the spectra preserve the character indicated in Fig. 1(a); however, the effect of increasing q vector on the L^- mode (Landau damping) (Refs. 7 and 8) starts becoming important. In addition, the photoluminescence background strongly increases, thus making the evaluation of the scattered intensity more difficult. In fact, Raman features become completely indistinguishable from the background in the configuration (y,x) for $\hbar\omega_L > 1.92$ eV. We note that a similar effect was also observed for plasmons in the (y,x) configuration at the E_1 gap in GaSb, where the photo-

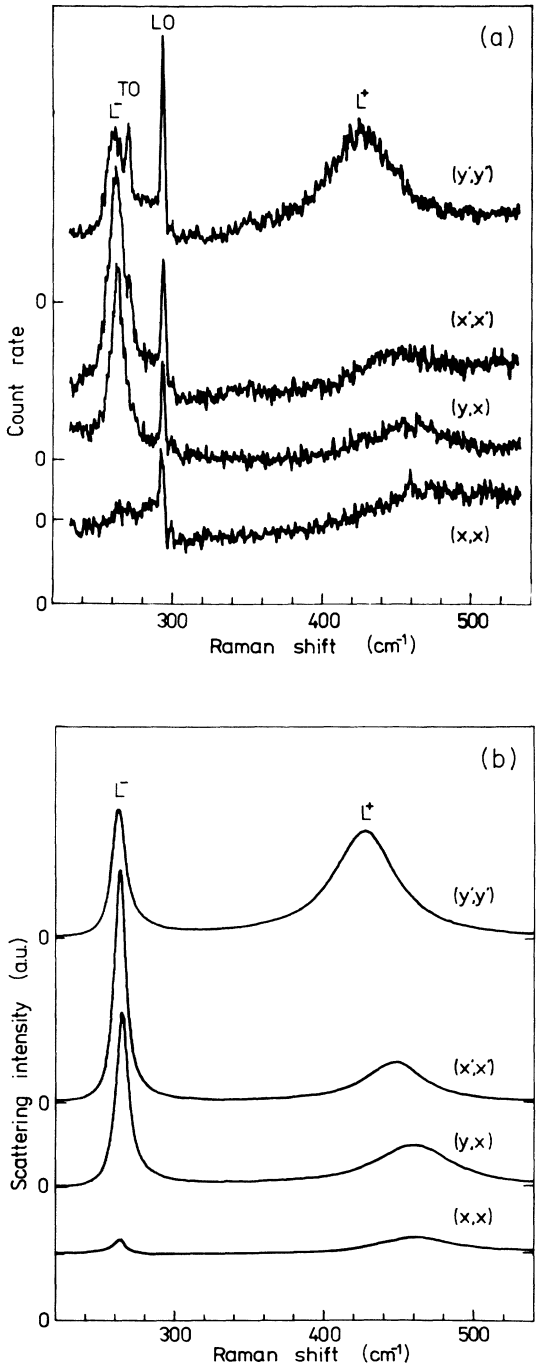

FIG. 1. (a) Experimental and (b) calculated Raman spectra of the investigated samples of n-type GaAs in the four configurations (1) at $\hbar\omega_L = 1.8$ eV and $T = 100$ K. For clarity, curves are displaced vertically.

luminescence background is less important.[2]

In Fig. 2 we show the resonance profiles of the Raman scattering efficiencies $dS/d\Omega$ (per unit length and unit solid angle) for the L^- and L^+ modes. No points are plotted for the configuration (y,x) above $\hbar\omega_L = 1.92$ eV, as the weak Raman features (three-band resonance[7]) were obscured by strong photoluminescence in this region. The resonance profiles are rather broad, the curves display the interferences clearly. Both (x',x') and (y',y') configurations dominate in scattering by the L^- mode, whereas the configuration (x',x') dominates for L^+. The resonance curves for the L^+ mode peak at slightly higher energies than those for L^- [with the exception of the (y',y') configuration]. There is a distinct difference between the profiles for the (x',x') and (y',y') configurations, and a slight shift in the positions of their maxima for the L^- mode, whereas for L^+ the maximum in configuration (y',y') is simply lower and broader than that for (x',x'). The maxima for configuration (x,x) are always lower than for configurations (x',x') and (y',y'). The resonance maxima in the L^+ mode are 2–5 times larger than their counterparts in the L^- mode.

The Raman efficiencies of Fig. 2 were converted to the squared Raman polarizabilities, treating L^- as a pure phonon and L^+ as a pure plasmon. We recall that the Raman polarizability $a \sim \bar{u}_0^{-1}$, where $\bar{u}_0$ is the zero-point amplitude of the relative displacement of the longitudinal mode.[2] For n-type GaAs with $N = 1.5\times10^{18}$ cm^{-3}, the ratio $|a_P|^2/|a_{LO}|^2$ is 1.05×10^{-10}. The Raman polarizabilities obtained in this way are shown in Fig. 3. The assumption of complete phonon (plasmon) character of the L^- (L^+) mode is rather crude, as there is a distinct frequency difference between the TO (screened LO phonon) and L^- peaks [Fig. 1(a)]. In fact, the strength of L^- is overestimated in this way, whereas that of L^+ is underestimated. A rough correction is always possible by properly scaling the vertical axes according to the respective amounts of the phonon and plasmon strengths.

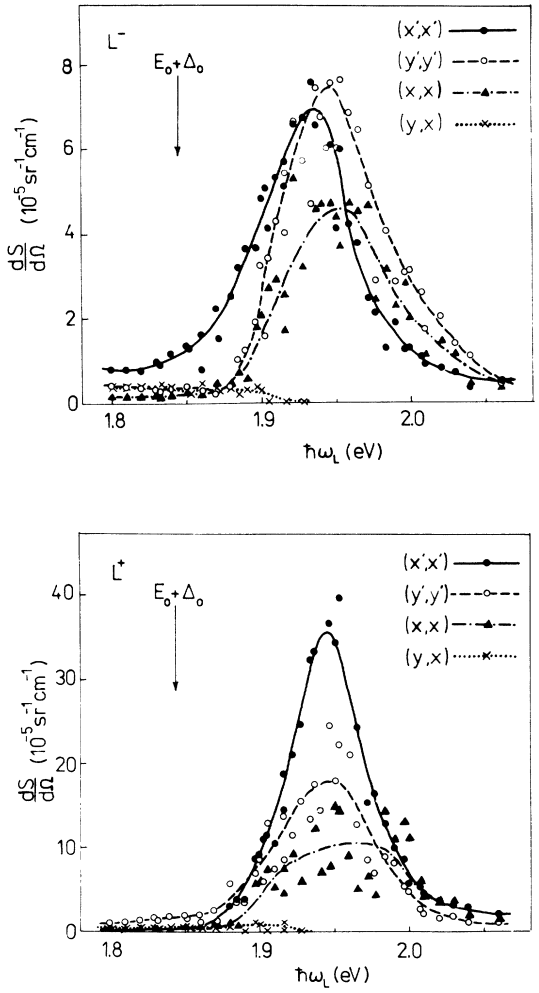

FIG. 2. Raman efficiencies for scattering by coupled plasmon–LO-phonon modes L^- and L^+ in n-type GaAs in configurations (1) determined for the samples of Table I. The lines are a guide to the eye.

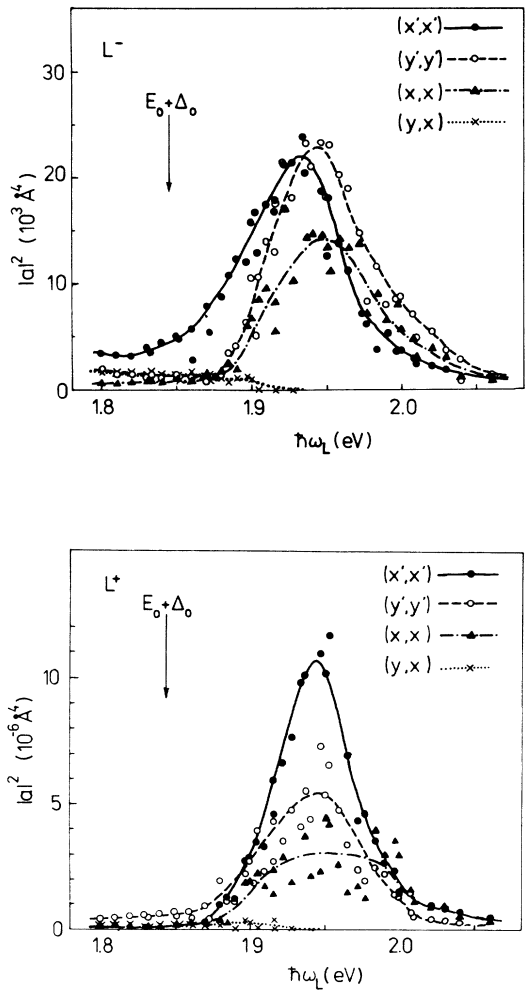

FIG. 3. Squared Raman polarizabilities for scattering by coupled plasmon–LO-phonon modes L^- and L^+ in n-type GaAs in configurations (1) determined for the samples of Table I. The lines are a guide to the eye.

IV. DISCUSSION AND CONCLUSIONS

A. Modeling procedure

The model spectra were calculated using Eq. (2). The spectral lines obtained in this way were integrated numerically to get the resonance behavior of the squared Raman polarizabilities. The expressions for DP (+EO) and F scattering given in Ref. 12 were used in the calculations. The parameters A_1, A_2, and A_3 in the DP mechanism were chosen so as to reproduce the Raman polarizability of pure GaAs (Ref. 10) in the intrinsic limit ($\bar{E}_0 \rightarrow E_0$). The prefactor for the F mechanism was enhanced to yield a contribution comparable with that of CDF's at resonance, as suggested in Ref. 8. This contribution was calculated with use of Eq. (5). Contrary to the other mechanisms, only the incoming resonance was taken into account; the outgoing resonance for the coupled modes was estimated to be at least 5 times smaller than the in-going one,[7,8] and, also, the analysis of experimental data in Ref. 9 does not indicate its presence. Impurity-induced scattering was not explicitly included in the calculations. This is, of course, a rough approximation. Recent calculations for undoped samples which include excitonic effects[16] suggest that impurity effects may be weaker than previously thought.[1] Impurity-induced scattering was, however, invoked in discussing the presence of the TO peak, in the experimental spectra [Fig. 1(a)]. On the other hand, owing to the presence of the electron plasma, the impurity potential should be screend out in the bulk, remaining strongly effective in the depleted surface layer.

The effective gap E_G has been evaluated, taking both the conduction-band nonparabolicity[17] and valence-band curvature into account. $\bar{E}_0$ was then approximated by $\bar{E}_0 = E_G - \Delta_0$. The effective broadening η_G was estimated, taking into account both the damping of the plasma, Γ, and the additional doping-induced broadening $\Delta\eta$: $\eta_G = \eta_{E_0+\Delta_0} + \Gamma + \Delta\eta$. The value $\eta_{E_0+\Delta_0} = 8$ meV has been taken from Ref. 1, $\Gamma = 7.5$ meV. To our knowledge, no study of the influence of doping on the broadening of the $E_0+\Delta_0$ gap has been performed. Therefore, considering the analogy between GaAs and Ge, we estimated the increase of broadening due to the doping as $\Delta\eta \sim 2.5$ meV, using known data for higher gaps in Ge.[18,19]

B. Spectral profiles

Spectra calculated for the four configurations (1) by means of Eq. (2) are displayed in Fig. 1(b). Satisfactory agreement is found with the experimental curves. The calculated positions of the L^- and L^+ peaks coincide with the experimental ones within 1 cm^{-1}, and, also, the line shapes are reasonably reproduced, especially for the L^+ feature. The electron concentrations and plasma-damping constants determined for the three samples from the observed positions of the L^+ modes are listed in Table I. Certain inhomogeneous distributions of carrier concentration in the wafer used, also indicated by ir reflectivity, are clearly seen. Despite this fact, interesting information may be drawn from the spectra.

First, the relation of the L^- and L^+ peak intensities in configuration (y,x) is, besides the values of N and $\hbar\omega_L$, essentially influenced by the relative strengths of the DP and E_0 contributions, i.e., by the Faust-Henry coefficient, C_{FH} (cf., e.g., Ref. 6). Its magnitude in intrinsic GaAs was estimated to be $|C_{FH}| = 0.6 \pm 0.2$ (Ref. 20) and 0.39 ± 0.02 (Ref. 21) below E_0 and near $E_0+\Delta_0$, respectively. In the main absorption region, C_{FH} must be complex, as pointed out in Ref. 2. We have found the value $C_{FH} = \mp 0.6 \pm 10.16$ to account for the spectrum of Fig. 1(a) in configuration (y,x). Allowing for an uncertainty of ± 0.2 in the real part of C_{FH}, as estimated from our fit, this value compares reasonably well with both published ones.

Second, the constant term in Eq. (5) was determined to be $A = 14 \pm 2$ Å^2. Without it, the model spectrum in the configuration (x,x) would be too weak, and no difference among the configurations (x',x'), (y',y'), and (y,x) (i.e., no interference) would exist, contrary to the experimental results. This is due to the fact that the contributions from the E_0 and E_G gaps almost cancel at $\hbar\omega_L = 1.8$ eV. We note that within the framework of our model the same (finite) value of A accounts reasonably for the

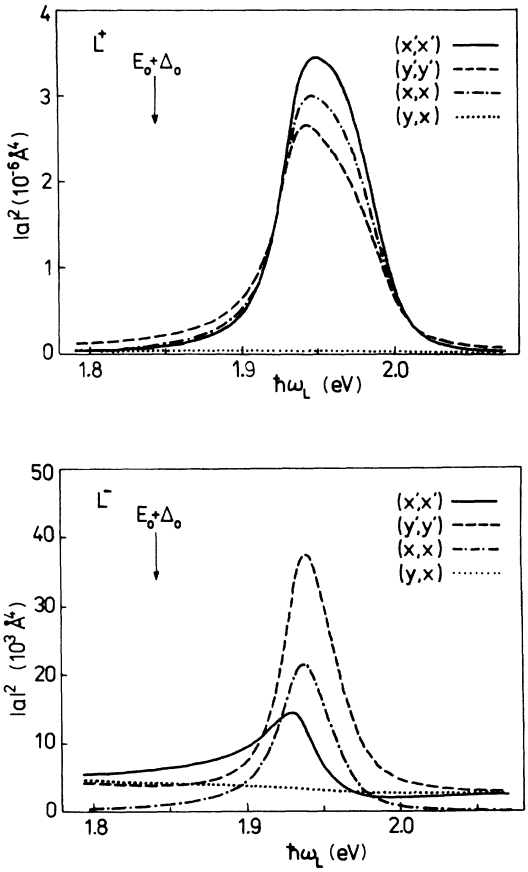

FIG. 4. Squared Raman polarizabilities for scattering by coupled plasmon–LO-phonon modes L^- and L^+ in n-type GaAs in configurations (1). Model curves calculated for $N = 1.5 \times 10^{18}$ cm^{-3} and $\Gamma = 7.5$ meV. [$m_c = 0.076 m_0$ (Ref. 13), $E_G = 1.937$ eV, and $\eta_G = 18$ meV.]

different intensities of the L^- and L^+ modes in the (y,z) and (z,z) polarizations well below the gap of GaAs (cf. Fig. 4 and related references in Ref. 6). Possible physical implications of this constant term in the CDF mechanism merit further investigation.

C. Resonance profiles

The model resonance profiles calculated for $N=1.5\times10^{18}$ cm^{-3} are shown in Fig. 4. The pure phonon (plasmon) character of the L^- (L^+) mode when only the DP (EO) mechanism is effective[2] was assumed in the calculations. The scaling between $|a_P|^2$ and $|a_{LO}|^2$ already used when calculating the experimental Raman polarizabilities was taken into account. The squared model Raman polarizabilities are of the same order of magnitude as the experimental ones. Comparing the sequence of the model resonance profiles with those measured (Fig. 3), one notices at once a close similarity below the maxima, a reasonable correspondence above them, and a clear discrepancy immediately around the maxima. This is not surprising since the CDF mechanism should dominate the scattering at the maxima, and it is well known that Eq. (5) is expected to give reasonable results only if $|E_G-\hbar\omega_L+i\eta_G|>\hbar\Omega$.[7] We shall discuss these similarities and differences in some detail.

The calculated resonance profiles are narrower than the measured ones. This is particularly striking for configuration (x,x). [The only exception is configuration (x',x') of the L^+ mode.] Also, the maxima of the curves calculated for this configuration always lie between the curves for configurations (x',x') and (y',y'). On the other hand, the maxima of configurations (x',x') and (y',y') for both modes are reproduced to within 5 meV. This is a very reasonable correspondence, as no adjustment of the peak positions was done when calculating the model curves. For the L^+ mode configuration (x',x') dominates among the calculated resonance profiles, as it is also the case in experiment. For the L^- mode configuration (y',y') dominates in the model, whereas the experimental maxima have nearly the same height for both configurations (x',x') and (y',y').

It might seem that the inclusion of impurity-induced scattering, an outgoing resonance in the CDF mechanism, and/or the apparent cancellation of the DP (+EO) mechanism for $\hbar\omega_L>1.9$ eV, as indicated by Figs. 2 and 3, should improve the agreement. However, this is not the case. We remind the reader that impurity-induced scattering adds to the intrinsic scattering incoherently,[10,12] thus increasing the total intensity of the scattering in the diagonal [(x',x'), (y',y'), and (x,x)] configurations and leaving the sequence of the curves unaltered. Hence, the different sequence of experimental maxima, as well as the different widths of the individual experimental curves, cannot be obtained in this way. Also, the explicit incorporation of the outgoing resonance into the CDF mechanism does not help. Being much weaker than the incoming one, it changes the resulting line shapes only slightly. On the other hand, the assumption that both resonances are comparable would influence the resonance profiles drastically: a pronounced two-peak structure would appear in the resonance profiles in all three diagonal configurations (especially for the L^- mode), unless very large damping, η_G, is assumed. However, no improvement of the agreement between the model and experimental curves can be achieved in this way either: the resonance maxima for the (x',x') [(y',y')] configuration of L^+ (L^-) mode are then shifted considerably towards higher energies. Of course, there is really no physical reason to increase the η_G value any further. The estimate of the strength of the outgoing resonance made in Ref. 8 thus appears to be strongly supported by this simple model.

Finally, a cancellation, if any, of the DP+EO mechanism at higher energies would result simply in the merging of the curves for all the diagonal configurations: without the DP+EO mechanism, no interference is possible. Indeed, the distinct interference observed experimentally at $\hbar\omega_L>1.95$ eV (especially for the L^- mode) indicates that the DP+EO contribution becomes less important, but does not cancel. This is also evidenced in other experiments.[9,22] Obviously, a suppression of the DP+EO contribution at higher energies would result in a closer correspondence between the model and measured profiles not only in this region. It would also ensure a closer correspondence of the absolute values of $|a|^2$ for configuration (y,x) and increase the height of the maximum of the curve (x',x') in the L^- mode. However, this latter achievement would be accompanied by an undesired increase of the maxima of the curves (y',y') and (x,x) for the L^+ mode. The results thus indicate that the functional dependence for the DP+EO scattering, which works very well for phonons, should be modified for the case of the coupled modes, even if the L^- mode is treated as a pure phonon. The reason obviously rests in the fact that the quasiparticles participating in the scattering process (electrons and coupled modes) are not independent near the $E_0+\Delta_0$ gap, as the electrons also take part in the formation of the coupled plasmon–LO-phonon modes. Attempts to improve the fit by including other *adjustable* parameters in the model expressions would not be, at this point, very informative.

There is very good correspondence between the model and the experimental data for configuration (y,x) over the entire interval in which the Raman peaks were resolved. However, the model values are systematically larger (smaller) for the L^- (L^+) mode (4.6×10^3 Å^4 versus 1.6×10^3 Å^4, and 3.5×10^{-8} Å^4 versus 1.3×10^{-7} Å^4 at $\hbar\omega_L=1.8$ eV). This is a direct consequence of our treatment of the L^- (L^+) mode as a pure phonon (plasmon) that overestimates (underestimates) the value of the Raman polarizability of the L^- (L^+) mode. Therefore, we consider this agreement satisfactory. In addition, it is well established for the case of LO phonons that the absolute values of the measured squared Raman polarizability in the allowed (y,x) configuration depend on the quality of the sample (cf. Figs. 2 and 3 of Ref. 1 and Fig. 2 of Ref. 10): $|a|^2$ increases with increasing sample perfection. Also, the expected interference effects of LO phonons have been observed most markedly on the high-purity liquid-phase-epitaxy–grown samples,[1,10] whereas commercial intrinsic substrates showed only

broad maxima.[1] A high concentration of uncontrolled impurities in commercial samples thus obscures the intrinsic effects.

For further progress in understanding the nature of interference effects in *n*-type GaAs, the investigation of doped samples with a high degree of perfection produced by advanced epitaxial technologies appears to be essential. Of course, a more sophisticated theoretical model going beyond the semiclassical approach used here is necessary. In particular, the fact that the quasiparticles participating in the process (electrons and coupled modes) are not independent near the $E_0+\Delta_0$ gap—since the electrons also take part in the formation of the coupled plasmon–LO-phonon modes—should be taken into account. Also, the treatment of coupled plasmon-phonon modes in the decoupled limit should be avoided.

To summarize, we have performed a detailed study, chiefly experimental, of the interference effects in resonant Raman scattering by coupled plasmon–LO-phonon modes in *n*-type GaAs near the $E_0+\Delta_0$ gap. We were able to describe quantitatively the measured spectra and resonance profiles below the resonance using the semiclassical dielectric theory of Raman scattering. The reason for the failure of this model at the resonance itself is probably only partly due to its inadequacy. Interference effects may be obscured by imperfections in the sample used. The strong photoluminescence background also decreases the accuracy of the Raman-scattering intensity determination.

ACKNOWLEDGMENTS

We gratefully acknowledge the expert technical assistance of M. Siemers, H. Hirt, and P. Wurster. We also thank A. Breitschwerdt and W. König for the infrared-reflectivity measurements. One of us (V.V.) is obliged to the Max-Planck-Gesellschaft for supporting his stay at the Max-Planck-Institut.

[1] J. Menéndez and M. Cardona, Phys. Rev. B **31**, 3696 (1985).
[2] W. Kauschke, N. Mestres, and M. Cardona, Phys. Rev. B **36**, 7469 (1987).
[3] W. Kauschke and M. Cardona, Phys. Scr. **T25**, 201 (1989).
[4] A. Cantarero, C. Trallero-Giner, and M. Cardona, Phys. Rev. B **39**, 8388 (1989); C. Trallero-Giner, A. Cantarero and M. Cardona, *ibid.* **40**, 4030 (1989).
[5] M. V. Klein, B. N. Ganguly, and P. J. Colwell, Phys. Rev. B **6**, 2380 (1972).
[6] M. V. Klein, in *Light Scattering in Solids I,* Vol. 8 of *Topics in Applied Physics,* edited by M. Cardona (Springer, Berlin, 1983), p. 147.
[7] G. Abstreiter, A. Pinczuk, and M. Cardona, in *Light Scattering in Solids IV,* Vol. 54 of *Topics in Applied Physics,* edited by M. Cardona and G. Güntherodt (Springer, Berlin, 1983), p. 5.
[8] A. Pinczuk, G. Abstreiter, R. Trommer, and M. Cardona, Solid State Commun. **30**, 429 (1979).
[9] C. Y. Chen, Phys. Rev. B **27**, 1436 (1983).
[10] W. Kauschke, M. Cardona, and E. Bauser, Phys. Rev. B **35**, 8030 (1987).
[11] U. Nowak, W. Richter, and G. Sachs, Phys. Status Solidi B **108**, 131 (1981).
[12] W. Kauschke and M. Cardona, Phys. Rev. B **33**, 5473 (1986).
[13] R. T. Holm, J. W. Gibson, and E. D. Palik, J. Appl. Phys. **48**, 212 (1977).
[14] J. Wagner and M. Cardona, Solid State Commun. **48**, 301 (1983).
[15] D. Olego and M. Cardona, Phys. Rev. B **24**, 7217 (1981).
[16] A. Cantarero, C. Trallero-Giner, and M. Cardona, Phys. Rev. B **40**, 12 290 (1989).
[17] D. Julienne, F. Le Saos, A. Fortini, and P. Bauduin, Phys. Rev. B **13**, 2576 (1976).
[18] A. K. Sood, G. Contreras, and M. Cardona, Phys. Rev. B **31**, 3760 (1985).
[19] L. Viña and M. Cardona, Phys. Rev. B **34**, 2586 (1986).
[20] A. K. Sood, W. Kauschke, J. Menéndez, and M. Cardona, Phys. Rev. B **35**, 2886 (1987).
[21] J. Biellmann, B. Prevot, and C. Schwab, J. Phys. C **16**, 1135 (1983).
[22] V. Vorlíček and I. Gregora (unpublished).